Geophysical Research Letters

RESEARCH LETTER
10.1029/2020GL091875

# Impact of Amazonian Fires on Atmospheric $CO_2$

**Xun Jiang[1], King-Fai Li[2], Mao-Chang Liang[3], and Yuk L. Yung[4,5]**

[1]Department of Earth and Atmospheric Sciences, University of Houston, Houston, TX, USA, [2]Department of Environmental Sciences, University of California, Riverside, CA, USA, [3]Institute of Earth Sciences, Academia Sinica, Taipei, Taiwan, [4]Division of Geological and Planetary Sciences, California Institute of Technology, Pasadena, CA, USA, [5]Jet Propulsion Laboratory, Pasadena, CA, USA

**Key Points:**

- $CO_2$ concentrations are higher over the Amazon than the surrounding region during the fire/dry season
- High concentrations of $CO_2$ are related to the biomass burning, enhanced sinking air, and surface winds
- Amazon forest changes from a $CO_2$ sink to a $CO_2$ source during the fire season

**Supporting Information:**

- Supporting Information S1

**Correspondence to:**
Y. L. Yung,
yly@gps.caltech.edu

**Citation:**
Jiang, X., Li, K.-F., Liang, M.-C., & Yung, Y. L. (2021). Impact of Amazonian fires on atmospheric $CO_2$. *Geophysical Research Letters*, *48*, e2020GL091875. https://doi.org/10.1029/2020GL091875

Received 1 DEC 2020
Accepted 4 FEB 2021

**Abstract** Amazon rainforest fires have significant environmental and societal impacts, but the mechanism and impact of the fires on the regional and global carbon cycles have not been fully understood. Over the rainforest, less precipitation, higher surface temperature, and enhanced mid-tropospheric sinking air over the eastern part of the Amazon characterized the fire/dry season. These meteorological conditions will facilitate more fires in the Amazon rainforest. Using the Orbiting Carbon Observatory-2 column $CO_2$, we notice that there are ~2 ppm more $CO_2$ over the Amazon compared with the surrounding area during the fire season. The higher concentrations of atmospheric $CO_2$ are related to the surface biomass burning, enhanced sinking air over the eastern part of the Amazon, and surface winds. Results from this study can help us better understand the carbon sources and sinks over the Amazon during the fire/dry season.

**Plain Language Summary** In this study, we explore the influence of fires on atmospheric $CO_2$ over the whole Amazon region using satellite $CO_2$ data. Our analysis not only reveals an increase in the $CO_2$ concentration (~2 ppm) over the Amazon during the fire season but also provides a possible mechanism to explain the increase. Our study further suggests that the Amazon forest changes from a $CO_2$ sink to a $CO_2$ source during the fire season. The increase in the $CO_2$ can lead to a warmer climate and produce more fires. It is still a challenge for current models to simulate the impact of fires on atmospheric $CO_2$ correctly, especially the interannual variability. Results in this study can help us better constrain models in the future.

## 1. Introduction

The Amazon rainforest is the largest biospheric carbon sink (e.g., Hubau et al., 2020; Pan et al., 2011) and is home to 10%–15% of terrestrial biodiversity (da Silva et al., 2005). However, as of 2018, ~20% of the Brazilian Amazon, which contains ~60% of the Amazon Basin, has been deforested (da Cruz et al., 2020), primarily for subsistence activities, soybean planting, cattle raising, timber logging, and mineral mining. During 2005–2012, the deforestation rate of the Brazilian Amazon significantly dropped by 70% compared to the record in 2004 after a series of national and international efforts, such as satellite monitoring (Diniz et al., 2015), increased state-protected forest areas (Walker et al., 2020), supply chain governance (Nepstad et al., 2014), and intergovernmental agreements (Simonet et al., 2019). However, the trend was first flattened and then reversed after the easing of Brazil's Forest Code in 2012 (Soares-Filho et al., 2014) and 2018 (Abessa et al., 2019); the deforestation in the last two years has been more severe due to the recent increased exports of agricultural products (Fuchs et al., 2019). The deforestation rate of the Brazilian Amazon has now surpassed the level in 2008 and the rate is still accelerating as of the summer of 2020.

Biomass burning, often associated with forest clearing, converts the carbon stored in the vegetative biomass mostly into atmospheric carbon dioxide ($CO_2$) and carbon monoxide (CO) (Guyon et al., 2005). Thus, deforestation has at least two distinct impacts on climate. The first impact is the increase of radiative forcing resulting from the direct increase of atmospheric $CO_2$. The second is the indirect influence through a subtle alteration of the hydrological cycle due to the changes in the surface types (e.g., from a forest to bare surface or from trees to savannas) and the atmospheric vertical structure.

The hydrologic cycle over the Amazon Basin is sensitive to the changes in the forest cover and the temperature near the surface. Barkhordarian et al. (2018) showed that as the northern South America becomes

warmer in response to anthropogenic forcing (e.g., greenhouse gases and anthropogenic aerosols), the surface and the atmosphere become drier (Barkhordarian et al., 2019; Berg et al., 2016; Trenberth et al., 2014). The increasingly dry conditions would in turn increase the frequency and extend the lifespan of the wildfires, further reducing forested areas, releasing more $CO_2$, enhancing greenhouse warming, and eventually risking the very existence of the rainforests (Brando et al., 2020; Khanna et al., 2017; Marengo et al., 2011).

Our knowledge about the $CO_2$ release from the Amazon rainforest, however, has been limited due to the lack of long-term measurements of $CO_2$ concentrations and fluxes over the whole Amazon region (Pastorello et al., 2020). Satellite observations of mid-tropospheric $CO_2$ (Chahine et al., 2008; Crevoisier et al., 2009; Kulawik et al., 2010; Rinsland et al., 2010) and column $CO_2$ (Crisp et al., 2012; Shiomi et al., 2008) have revealed important natural $CO_2$ variability over the global domain, such as Madden–Julian Oscillation (Li, 2018; Li et al., 2010), stratospheric sudden warming (Jiang et al., 2013), monsoon (e.g., Wang et al., 2011), El Niño (e.g., Chatterjee et al., 2017), annular mode (Jiang et al., 2010), and volcano eruption (Schwandner et al., 2017). Satellite $CO_2$ measurements are capable of detecting the enhanced $CO_2$ emissions from wildfires over Indonesia (Heymann et al., 2017) and southern California (Li et al., 2019). Over the Amazon region, a previous study using aircraft data found that more $CO_2$ was released to the atmosphere during wildfires (Guyon et al., 2005). Using bi-weekly vertical profiles of $CO_2$ from the surface to 4.4 km at four locations over the Amazon basin, Gatti et al. (2014) noticed that carbon was lost from the Amazon basin as a response of stalled forest productivity and wildfires during dry years. Previous studies (e.g., Gatti et al., 2014; Guyon et al., 2005) are limited in space and cannot provide a full picture of the impact of fires on atmospheric $CO_2$ over the whole domain of the Amazon. Satellite $CO_2$ data are global, so a systematic comparison of atmospheric $CO_2$ between Amazon and the surrounding areas can be conducted. Below, we utilize the satellite $CO_2$ observations from National Aeronautics and Space Administration (NASA) Orbiting Carbon Observatory-2 (OCO-2) mission to investigate the impacts of fires on atmospheric $CO_2$ over the whole Amazon region.

## 2. Data

### 2.1. Precipitation Data

Global Precipitation Climatology Project (GPCP) Version 2.3 precipitation (Adler et al., 2018), National Centers for Environmental Prediction Reanalysis 2 (NCEP2) surface temperature, NCEP2 500 hPa vertical pressure velocity, NCEP2 surface pressure, and NCEP2 surface winds (Kanamitsu et al., 2002) are used in this paper to study the meteorological conditions for fires in the Amazon. Monthly mean GPCP Version 2.3 precipitation data and NCEP2 data are available from January 1979 to present. The spatial resolution of GPCP Version 2.3 precipitation data and NCEP2 data are 2.5° × 2.5° in latitude and longitude.

### 2.2. OCO-2 and AIRS Data

To explore the impact of Amazon fires on atmospheric $CO_2$, we have utilized Version 9 OCO-2 column $CO_2$ (Crisp et al., 2017; Eldering et al., 2017) in this paper. We also use Version 6 column CO data from Atmospheric Infrared Sounder (AIRS) (Warner et al., 2013; Yurganov et al., 2008), because CO data can be used to track biomass burning events (Yurganov et al., 2008). OCO-2 column $CO_2$ data are retrieved using $CO_2$ spectra at 1.61 and 2.06 $\mu$m (Connor et al., 2008; Crisp et al., 2017). Comparisons between OCO-2 column $CO_2$ and in-situ measurements from Total Carbon Column Observing Network (TCCON) suggest that the precision of OCO-2 column $CO_2$ is about 0.5 ± 1.5 ppm (Wunch et al., 2017). OCO-2 column $CO_2$ data are available from September 2014 to present. AIRS column CO has a maximum sensitivity at 500 hPa. AIRS column CO data are available from September 2002 to present. In this paper, we have regridded OCO-2 column $CO_2$ and AIRS column CO to 2° × 2° in latitude and longitude.

### 2.3. Fire Emission Database

To better understand the impact of $CO_2$ surface emissions on atmospheric $CO_2$ during the fire season in the Amazon, we have utilized $CO_2$ biomass burning emissions from Global Fire Emissions Database Version 4.1 (GFEDv4.1) (Giglio et al., 2013) and biosphere $CO_2$ emissions from the Carnegie-Ames Stanford Approach

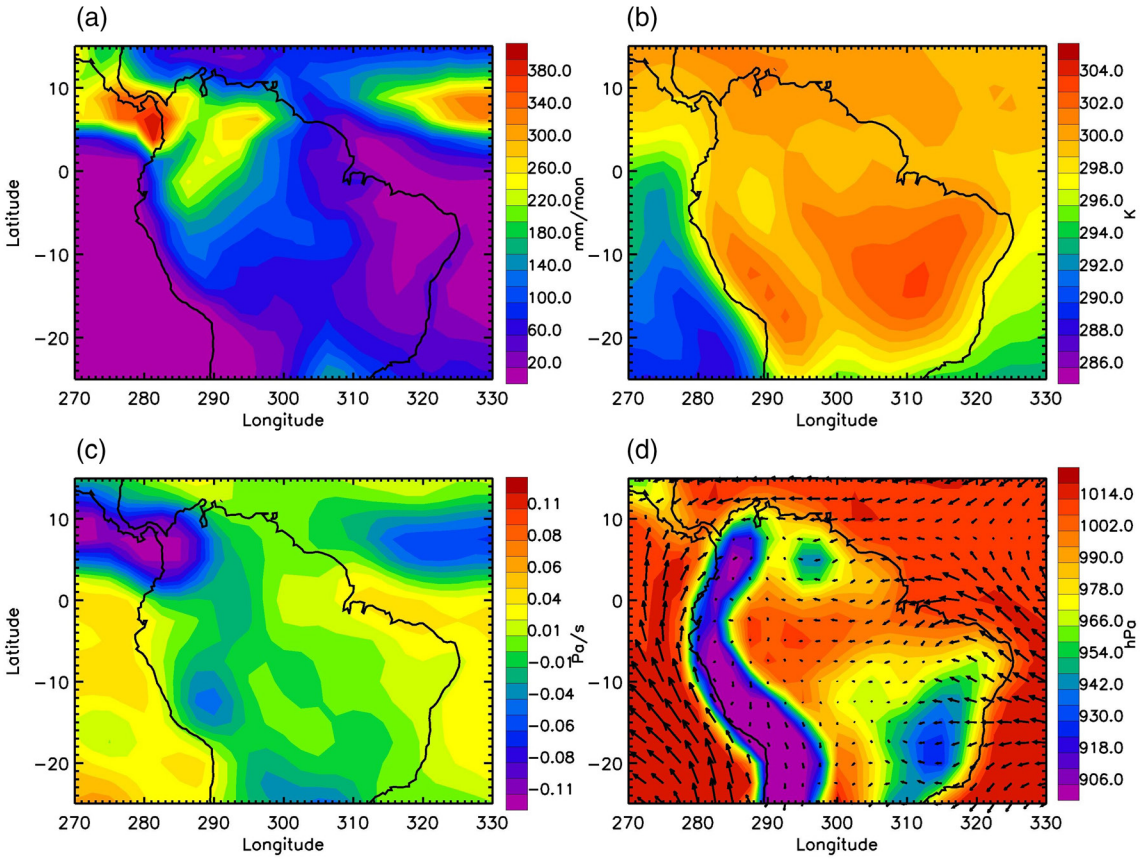


**Figure 1.** (a) Global Precipitation Climatology Project (GPCP) precipitation averaged for August–October, 2015–2019. Units are mm/mon. (b) NCEP2 surface temperature averaged for August–October, 2015–2019. Units are K. (c) NCEP2 500 hPa vertical pressure velocity averaged for August–October, 2015–2019. Units are Pa/s. (d) NCEP2 surface pressure and horizontal winds averaged for August–October, 2015–2019. Units for surface pressure are hPa.

(CASA) biogeochemical model (Randerson et al., 1996). Monthly mean GFEDv4.1 $CO_2$ biomass burning emissions and CASA biosphere-atmosphere $CO_2$ exchange data are available from January 1997 to December 2016. The spatial resolution of GFEDv4.1 biomass burning $CO_2$ emissions and CASA biosphere-atmosphere $CO_2$ exchange data are 0.25° × 0.25° in latitude and longitude. GFEDv4.1 $CO_2$ biomass burning data and CASA biosphere-atmosphere $CO_2$ exchange data are not available in later years (2017–2019) due to the inconsistency of upgraded burned area data (Randerson et al., 2018). We will revisit the $CO_2$ emission in the future when surface emission data are available in later years (2017–2019).

### 2.4. Burned Area Data

Burned area data from Moderate Resolution Imaging Spectrometer (MODIS) (Giglio et al., 2018) are also used in this paper. MODIS burned area data are available from November 2000 to December 2019. The spatial resolution of the monthly mean MODIS burned area are 0.25° × 0.25° in latitude and longitude.

## 3. Results

We focus on the period from August to October, the dry months of the Amazon, when the Amazon fires mostly occur. To investigate the meteorological conditions in the fire/dry season in the Amazon, we calculate mean values of Global Precipitation Climatology Project (GPCP) Version 2.3 precipitation, the National Centers for Environmental Prediction's Reanalysis 2 (NCEP2) surface temperature, NCEP2 500-hPa vertical pressure velocity, NCEP2 surface pressure, and NCEP2 surface horizontal winds over the fire/dry season from 2015 to 2019. Figure 1a shows that the amount of precipitation is low over the Amazon during the fire/dry season (August–October, 2015–2019). Surface temperature is high over the Amazon (see Figure 1b).

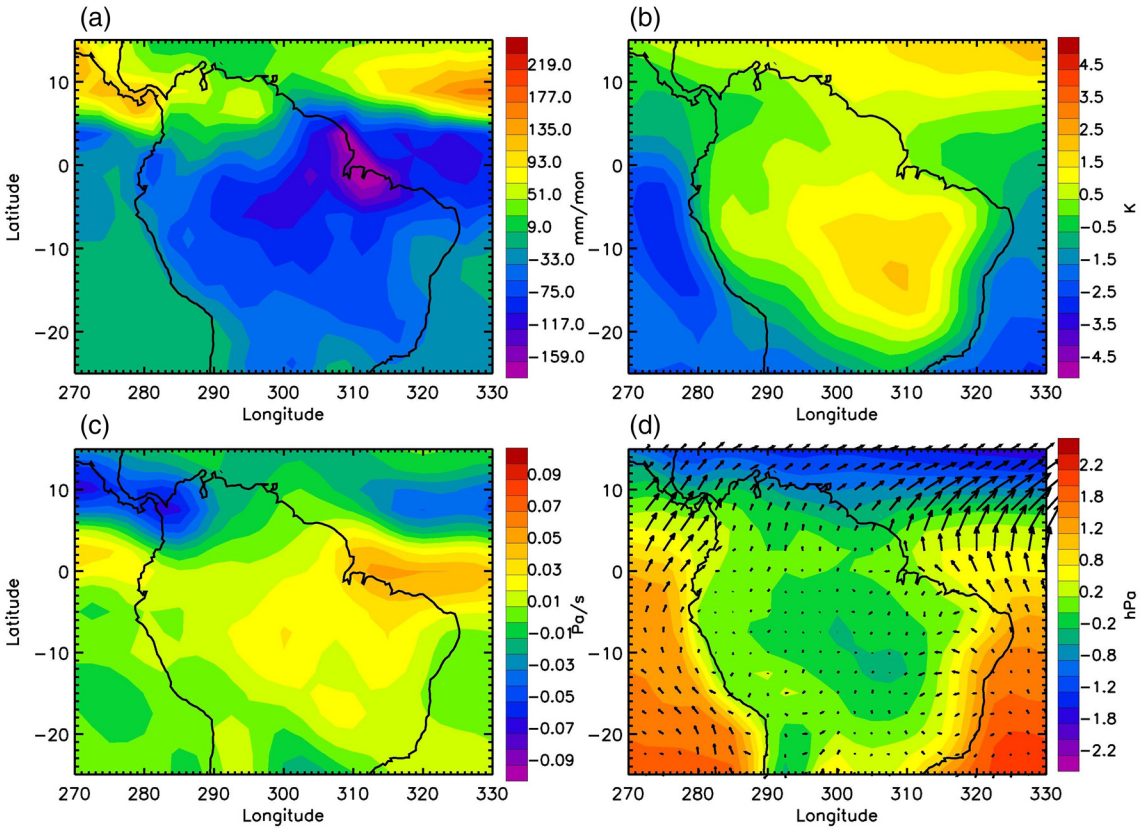


**Figure 2.** (a) GPCP precipitation anomaly for August–October, 2015–2019. Units are mm/mon. (b) NCEP2 surface temperature anomaly for August–October, 2015–2019. Units are K. (c) NCEP2 500 hPa vertical pressure velocity anomaly for August–October, 2015–2019. Units are Pa/s. (d) NCEP2 surface pressure anomaly and horizontal wind anomaly for August–October, 2015–2019. Units for surface pressure are hPa.

Figure 1c shows 500 hPa vertical pressure velocity averaged for the fire/dry season. Negative (positive) value of 500 hPa vertical pressure velocity refers to rising (sinking) air. There is rising air over the western part of South America and sinking air over the eastern part of South America. There is a low-pressure system in the western part of South America and a high-pressure system in the eastern part of South America (See Figure 1d). Surface winds move toward the Amazon basin from the east coast. With Andes Mountains along the west coast of South America, the westward winds from the east coast tend to trap pollutants released from the fires in the Amazon basin. Figure 2 shows the anomalies of GPCP precipitation, NCEP2 surface temperature, NCEP2 500-hPa vertical pressure velocity, and NCEP2 surface pressure and horizontal winds. Anomalies are calculated by subtracting the climatological averages (January 2015–December 2019) from original data at each grid point. The precipitation is anomalously less during the fire/dry season compared with climatology over the Amazon (Figure 2a), and is accompanied by a higher surface temperature and enhanced sinking air over the eastern Amazon. These meteorological anomalies would further enhance the fire frequency and intensity during the dry season. There is a small surface pressure anomaly (~0.5 hPa) as shown in Figure 2d, which is very small compared with the surface pressure (~950–1,000 hPa) in Figure 1d. There is also stronger converging air from west, east, and south directions, moving pollutants from the southern Amazon to the northern Amazon.

To investigate the impact of fires on atmospheric $CO_2$, we calculate the mean value of detrended OCO-2 column $CO_2$ in August–October, 2015–2019. Since we are not interested in the positive trend in column $CO_2$ in this study, a linear trend estimated by the least squares method (Bevington & Robinson, 2003) has been removed from OCO-2 column $CO_2$ data at each grid point. As shown in Figure 3a, $CO_2$ concentrations are about 2 ppm higher over the Amazon region than the surrounding areas. Since CO, produced by incomplete combustion, can track the biomass burning well (Yurganov et al., 2008), we also calculate the mean

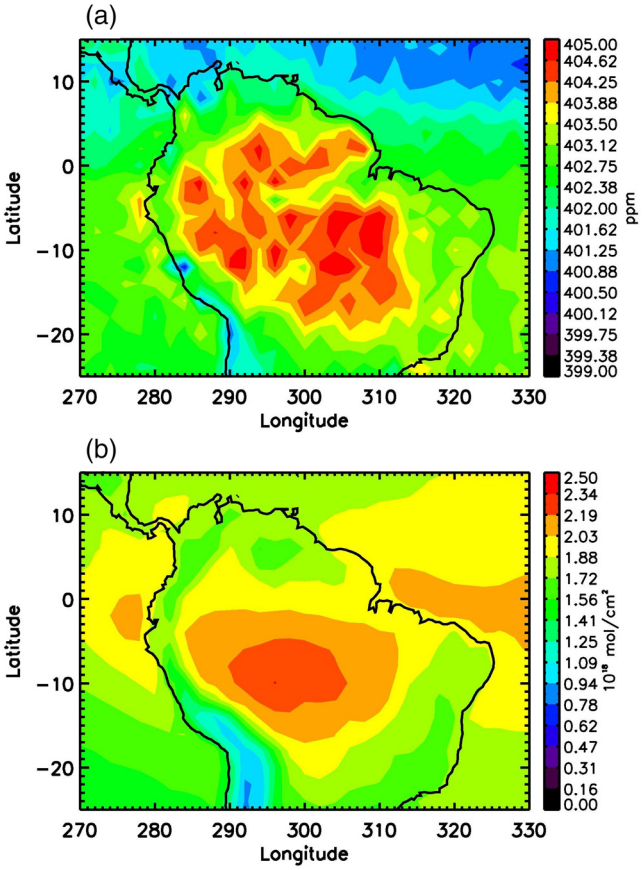


**Figure 3.** (a) OCO-2 $CO_2$ averaged for August–October, 2015–2019. Units are ppm. (b) Atmospheric Infrared Sounder (AIRS) column CO averaged for August–October, 2015–2019. Units are $10^{18}$ mol/cm$^2$.

value of AIRS column CO in August–October, 2015–2019. As shown in Figure 3b, CO concentrations are higher over the Amazon region than the surrounding areas.

To investigate possible explanations for the high atmospheric $CO_2$ concentrations over the Amazon during the fire/dry season, we examine surface $CO_2$ emissions over the Amazon using the global $CO_2$ biomass burning emission from the Global Fire Emissions Database, Version 4.1 (GFEDv4) and the net ecosystem $CO_2$ exchange (NEE), defined as the difference between respiration and gross primary production (photosynthesis), from the Carnegie-Ames-Stanford Approach (CASA) model. $CO_2$ surface emissions averaged in August–October, 2015–2016 are shown in Figure 4. For a direct comparison, we also calculate mean values of detrended OCO-2 column $CO_2$ and AIRS column CO during August–October, 2015–2016 in Figure S1. Figure 4a shows an enhanced $CO_2$ emission from biomass burning during the fire/dry season over the Amazon region, consistent with the OCO-2 observations. $CO_2$ biomass burning emissions are particularly high over the southern part of the Amazon. There are also elevated $CO_2$ biomass-burning emissions over the central and northern parts of the Amazon, which contributes to the high $CO_2$ concentration in the atmosphere as shown in Figure 3a. The positive values of NEE in Figure 4b suggest that $CO_2$ are released from the biosphere to the atmosphere; negative values of NEE suggest that $CO_2$ is removed from the atmosphere by the biosphere. Thus $CO_2$ is released from the biosphere to the atmosphere over the southern and northern parts of the Amazon during the fire/dry season while $CO_2$ is taken up in the northeastern and northwestern parts of the Amazon. Ecosystem respiration (ER) and gross primary production (GPP) averaged in the fire/dry season are shown in Figures 4c and 4d, respectively. The spatial distribution of $CO_2$ released from respiration is more uniform over the Amazon region than that of $CO_2$ uptake by photosynthesis. There is less $CO_2$ uptake by photosynthesis over the southern Amazon, where most fires occur. The combination of respiration and photosynthesis contributes to the enhanced $CO_2$ release in the southern and northern parts of the Amazon as shown in Figure 4b.

Figure S2 shows the anomalies of GFEDv4.1 biomass burning, NEE, ER, and GPP for August−October, 2015–2016. $CO_2$ biomass burning emissions are anomalously high over the southern and central Amazon during the fire/dry season compared with climatology (Figure S2a). NEE anomalies are higher over southern and northern parts of the Amazon during the fire/dry season compared with climatology as shown in Figure S2b. Figure S3 shows the MODIS burned area and anomalies for August−October, 2015–2019. A lot of areas were burned over the southern and central Amazon. The burned areas during the fire/dry season (August−October, 2015–2019) are much higher than the climatology (Figure S3b), implying more $CO_2$ emission due to biomass burning during August−October, 2015–2019.

To explore the temporal variations of different variables over the Amazon, we calculate GPCP Version 2.3 precipitation and NCEP2 500 hPa vertical pressure velocity for the wet season (January−March) and the dry season (August–October) over 288°E-314°E, 20°S-0°S. The region (288°E-314°E, 20°S-0°S) is chosen, since this is the area with high concentrations of $CO_2$ and CO. Time series of GPCP precipitation (green line) and NCEP2 500 hPa vertical pressure velocity (blue line) are shown in Figure 5a. The average amount of precipitation is above 250 mm during the wet season (January–March) and is below 100 mm during the dry season (August−October). The values of 500 hPa vertical pressure velocity are higher during dry season than the wet season. There is more sinking air (or, equivalently, less rising air) during the dry season than the wet season, which can help trap trace gases in the Amazon region during the dry season (August–October). The same averaging algorithms as GPCP precipitation data are applied to OCO-2 column $CO_2$, AIRS

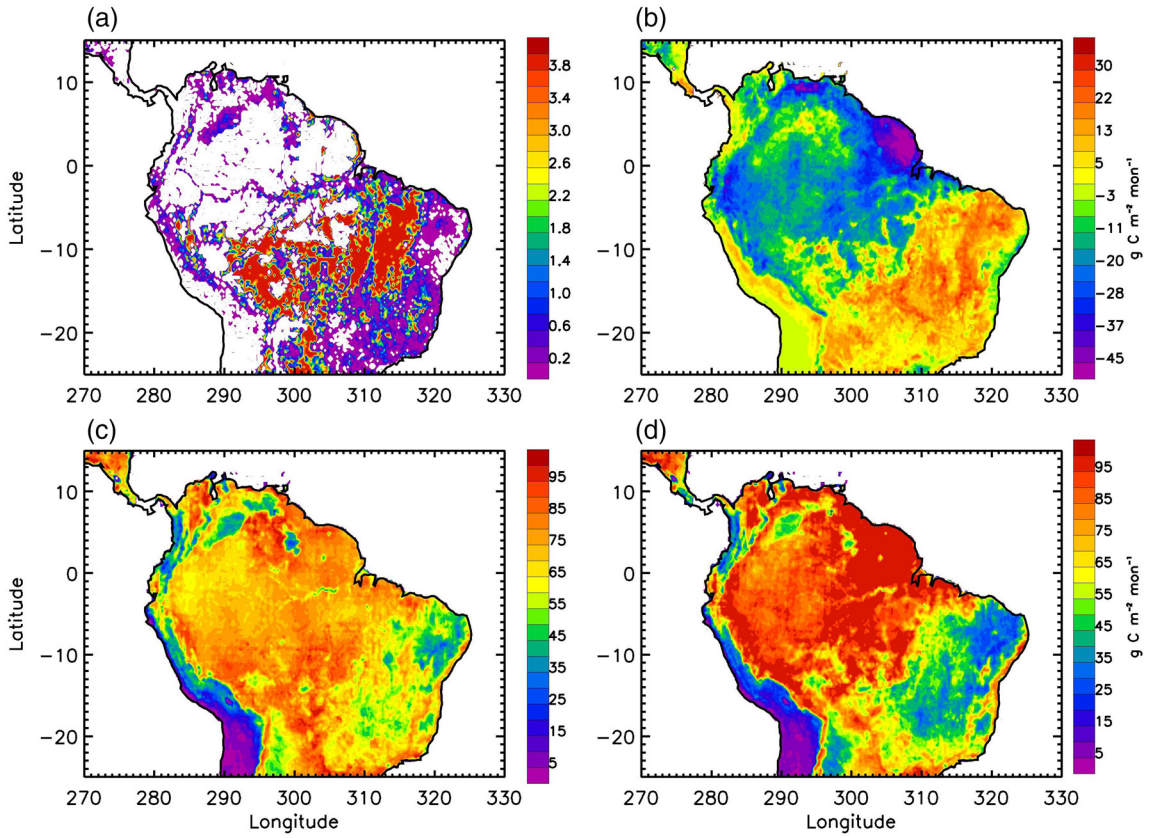


**Figure 4.** (a) GFEDv4.1 biomass burning averaged for August–October, 2015–2016. (b) Net ecosystem $CO_2$ exchange (NEE) averaged for August–October, 2015–2016. (c) Ecosystem respiration (ER) averaged for August–October, 2015–2016. (d) Gross primary production (GPP) averaged for August–October, 2015–2016. Units are g C $m^{-2}$ $mon^{-1}$.

column CO, and NEE. The black line is OCO-2 column $CO_2$ averaged over the region; the red line is AIRS column CO averaged over the region. Both CO and $CO_2$ released from the fire reflect the intensity of the fire. Figure 5b shows that the magnitudes of $CO_2$ and CO are comparable (high $CO_2$ coincides with high CO) except in 2016, where the $CO_2$ is influenced primarily by the biosphere's response to the strong El Niño event (Chatterjee et al., 2017; Levin et al., 2019; Liu et al., 2017). The correlation coefficient between OCO-2 column $CO_2$ and AIRS column CO is 0.74 with a significance level of 4%. The significance level is calculated using a Monte Carlo method (Jiang et al., 2004). Details for correlation coefficients and significance levels are summarized in Table S1 in supplementary materials. The correlation coefficients of GPCP precipitation with OCO-2 column $CO_2$ and AIRS CO are −0.65 (7%) and −0.95 (5%), respectively. Both OCO-2 column $CO_2$ and AIRS column CO concentrations are high during dry seasons (August–October) and low during wet seasons (January–March). The correlation coefficients of vertical pressure velocity with OCO-2 column $CO_2$ and AIRS CO are 0.64 (7%) and 0.95 (4%), respectively. More sinking air can contribute to more $CO_2$ and CO in the atmosphere during the dry season than the wet season. High concentrations of OCO-2 $CO_2$ during dry seasons (August–October) are also related to biomass burning and burned area as shown in Figures S4a and S4b, respectively. The anomalous signal in the wet season of 2016 is related to the strong 2015–2016 El Niño event (e.g., Chatterjee et al., 2017; Levine et al., 2019; Liu et al., 2017). The 2015–2016 El Niño event peaked in the late 2015 with severe droughts (Liu et al., 2017). Conditions of high surface temperature and low soil moisture lead to a reduction in the photosynthesis and an increase in the soil and plant respiration (Chatterjee et al., 2017; Levine et al., 2019; Liu et al., 2017), resulting in more $CO_2$ in the atmosphere. As shown as pink line in Figure 5b, the average value of NEE over the region (288°E-314°E, 20°S-0°S) is positive for January–March, 2016 which means more $CO_2$ is released from biosphere to the atmosphere as a response to the El Niño event. The average value of NEE over this region (pink line) is complex as a result of cancellation of positive and negative values over different regions (Figure 4b). The average value of

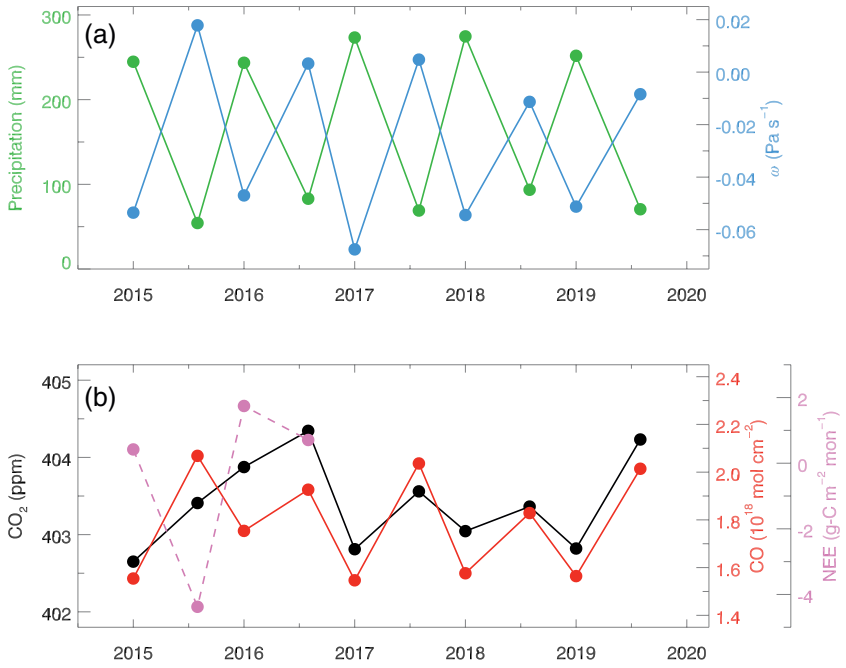


**Figure 5.** (a) Time series of GPCP precipitation and NCEP2 500 hPa vertical pressure velocity averaged over 288°E-314°E, 20°S-0°S for wet seasons (January–March) and dry seasons (August–October). Green line is precipitation and blue line is 500 hPa vertical pressure velocity. (b) Time series of detrended OCO-2 $CO_2$, AIRS column CO, and NEE averaged over 288°E-314°E, 20°S-0°S for wet seasons (January–March) and dry seasons (August–October). Black line is the detrended OCO-2 $CO_2$. Red line is AIRS column CO. Pink dashed line is NEE.

NEE is relatively small in the wet season (January–March) of 2015 and the dry season (August–October) of 2016. The average value of NEE is negative in the dry season (August–October) of 2015 which will be offset by the $CO_2$ biomass burning emission in the dry season of 2015 (Figure S4a in supplementary materials). The relatively high NEE during the wet season (January–March) of 2016 can help to explain the relatively high $CO_2$ concentration during the wet season (January–March) of 2016 as a response to the El Niño event.

## 4. Conclusions

In this paper, we have examined the impact of fires on atmospheric $CO_2$ over the Amazon region. To investigate the meteorological conditions during the fire/dry season, we calculate mean values and anomalies of precipitation, surface temperature, 500 hPa vertical pressure velocity, surface pressure, and surface winds during August–October, 2015–2019. There is less precipitation, higher surface temperature, and enhanced mid-tropospheric sinking air over the eastern part of the Amazon during the fire/dry season. All these meteorological conditions favor the formation of fires over the Amazon during the fire/dry season (August–October). To investigate the impacts of fires on atmospheric $CO_2$, we estimate concentrations of OCO-2 column $CO_2$ during the fire/dry season. Column $CO_2$ concentrations are about 2 ppm higher over the Amazon basin than the surrounding area during the fire/dry season, which coincides with a high column CO in the same region due to the incomplete combustion of the biomass, as observed by NASA's AIRS instrument. High concentrations of OCO-2 column $CO_2$ are related to the surface biomass burning, enhanced sinking air over the eastern part of the Amazon, and surface winds. Although the Amazon is the biggest land $CO_2$ sink, $CO_2$ released from fires make this region a $CO_2$ source during the fire/dry season (see Figure 4b), which will have a large impact on the carbon budget, leading to a warmer climate and more fires in the future.

Temporal variations of precipitation, vertical pressure velocity, OCO-2 column $CO_2$, AIRS CO, and MODIS burned area are also investigated. The time series of OCO-2 column $CO_2$ have a negative correlation with precipitation ($R = -0.65$) and positive correlations with vertical pressure velocity ($R = 0.64$), AIRS column CO ($R = 0.75$), and MODIS burned area ($R = 0.68$). It suggests that there is less precipitation, enhanced sinking air, and more burned area over the Amazon during the fire/dry season, which will contribute to

higher $CO_2$ concentrations. It remains challenging for biogeochemistry-transport models to simulate the impact of fires on atmospheric $CO_2$ correctly over the Amazon, especially the interannual variability. Results revealed from this study can help us better understand the carbon budget over the Amazon and constrain the numerical models. In the future, we plan to improve the aerosol retrievals and increase the yield of $CO_2$ retrievals over biomass-burning regions. With more yields over the biomass burning region and improved spatial coverage, we can explore the temporal variation of $CO_2$ during a biomass-burning event on a daily basis.

## Data Availability Statement

GPCP Version 2.3 precipitation data are available at https://psl.noaa.gov/data/gridded/data.gpcp.html. NCEP2 Reanalysis data are available at https://psl.noaa.gov/data/gridded/data.ncep.reanalysis2.html. OCO-2 Version 9 column $CO_2$ data are available at https://co2.jpl.nasa.gov/#mission=OCO-2. AIRS Version 6 column CO data are available at https://airs.jpl.nasa.gov/data/get-data/standard-data/. GFED Version 4.1 data are available at https://www.geo.vu.nl/~gwerf/GFED/GFED4/. MODIS burned area data are available at http://modis-fire.umd.edu/.

**Acknowledgments**
We thank R.-L. Shia for helpful comments. We thank two anonymous referees and the editor for their time and constructive suggestions. X. Jiang is supported by NASA ROSES Cassini Data Analysis Program. K.-F. Li is partially supported by NASA JPL Subcontracts 1631379 and 1653138. M.-C. Liang is supported by Ministry of Science and Technology, Taiwan (grant no. 108-2111-M-001-011-MY3) and Academia Sinica (grant no. AS-IA-109-M03). Y. L. Yung is supported by the NASA OCO-2 project.

## References

Abessa, D., Famá, A., & Buruaem, L. (2019). The systematic dismantling of Brazilian environmental laws risks losses on all fronts. *Nature Ecology & Evolution*, *3*(4), 510–511. https://doi.org/10.1038/s41559-019-0855-9

Adler, R. F., Sapiano, M. R. P., Huffman, G. J., Wang, J.-J., Gu, G., Bolvin, D., et al. (2018). The Global Precipitation Climatology Project (GPCP) monthly analysis (new version 2.3) and a review of 2017 global precipitation. *Atmosphere*, *9*(4), 138. https://doi.org/10.3390/atmos9040138

Barkhordarian, A., Saatchi, S. S., Behrangi, A., Loikith, P. C., & Mechoso, C. R. (2019). A recent systematic increase in vapor pressure deficit over tropical South America. *Scientific Reports*, *9*(1), 15331. https://doi.org/10.1038/s41598-019-51857-8

Barkhordarian, A., von Storch, H., Zorita, E., Loikith, P. C., & Mechoso, C. R. (2018). Observed warming over northern South America has an anthropogenic origin. *Climate Dynamics*, *51*(5–6), 1901–1914. https://doi.org/10.1007/s00382-017-3988-z

Berg, A., Findell, K., Lintner, B., Giannini, A., Seneviratne, S. I., van den Hurk, B., et al. (2016). Land–atmosphere feedbacks amplify aridity increase over land under global warming. *Nature Climate Change*, *6*(9), 869–874. https://doi.org/10.1038/nclimate3029

Bevington, P. R., & Robinson, D. K. (2003). *Data reduction and error analysis for the physical science* (3rd ed., p. 336). New York, NY, USA: McGraw-Hill.

Brando, P. M., Soares-Filho, B., Rodrigues, L., Assunção, A., Morton, D., Tuchschneider, D., et al. (2020). The gathering firestorm in southern Amazonia. *Science Advances*, *6*(2), eaay1632. https://doi.org/10.1126/sciadv.aay1632

Chahine, M. T., Chen, L., Dimotakis, P., Jiang, X., Li, Q., Olsen, E. T., et al. (2008). Satellite remote sounding of mid-tropospheric $CO_2$. *Geophysical Research Letters*, *35*(17), L17807. https://doi.org/10.1029/2008GL035022

Chatterjee, A., Gierach, M. M., Sutton, A. J., Feely, R. A., Crisp, D., Eldering, A., et al. (2017). Influence of El Niño on atmospheric $CO_2$ over the tropical Pacific Ocean: Findings from NASA's OCO-2 mission. *Science*, *358*(6360), eaam5776. https://doi.org/10.1126/science.aam5776

Connor, B. J., Boesch, H., Toon, G., Sen, B., Miller, C., & Crisp, D. (2008). Orbiting carbon observatory: Inverse method and prospective error analysis. *Journal of Geophysical Research*, *113*(D5), D05305. https://doi.org/10.1029/2006JD008336

Crevoisier, C., Chédin, A., Matsueda, H., Machida, T., Armante, R., & Scott, N. A. (2009). First year of upper tropospheric integrated content of $CO_2$ from IASI hyperspectral infrared observations. *Atmospheric Chemistry and Physics*, *9*(14), 4797–4810. https://doi.org/10.5194/acp-9-4797-2009

Crisp, D., Fisher, B. M., O'Dell, C., Frankenberg, C., Basilio, R., Bösch, H., et al. (2012). The ACOS $CO_2$ retrieval algorithm – Part II: Global $X_{CO2}$ data characterization. *Atmospheric Measurement Techniques*, *5*(4), 687–707. https://doi.org/10.5194/amt-5-687-2012

Crisp, D., Pollock, H. R., Rosenberg, R., Chapsky, L., Lee, R. A. M., Oyafuso, F. A., et al. (2017). The on-orbit performance of the Orbiting Carbon Observatory-2 (OCO-2) instrument and its radiometrically calibrated products. *Atmospheric Measurement Techniques*, *10*(1), 59–81. https://doi.org/10.5194/amt-10-59-2017

da Cruz, D. C., Benayas, J. M. R., Ferreira, G. C., Santos, S. R., & Schwartz, G. (2020). *An overview of forest loss and restoration in the Brazilian Amazon*. New Forests. Retrieved from https://doi.org/10.1007/s11056-020-09777-3

da Silva, J. M. C., Rylands, A. B., & da Fonseca, G. A. B. (2005). The fate of the Amazonian areas of endemism. *Conservation Biology*, *19*(3), 689–694. https://doi.org/10.1111/j.1523-1739.2005.00705.x

Diniz, C. G., Souza, A. A. D., Santos, D. C., Dias, M. C., da Luz, N. C., de Moraes, D. R. V., et al. (2015). DETER-B: The new Amazon near real-time deforestation detection system. *IEEE Journal of Selected Topics in Applied Earth Observations and Remote Sensing*, *8*(7), 3619–3628. https://doi.org/10.1109/JSTARS.2015.2437075

Eldering, A., O'Dell, C. W., Wennberg, P. O., Crisp, D., Gunson, M. R., Viatte, C., et al. (2017). The Orbiting Carbon Observatory-2: First 18 months of science data products. *Atmospheric Measurement Techniques*, *10*(2), 549–563. https://doi.org/10.5194/amt-10-549-2017

Fuchs, R., Alexander, P., Brown, C., Cossar, F., Henry, R. C., & Rounsevell, M. (2019). US–China trade war imperils Amazon rainforest. *Nature*, *567*(7749), 451–454. https://doi.org/10.1038/d41586-019-00896-2

Gatti, L. V., Gloor, M., Miller, J. B., Doughty, C. E., Malhi, Y., Domingues, L. G., et al. (2014). Drought sensitivities of Amazonian carbon balance revealed by atmospheric measurements. *Nature*, *506*(7486), 76–80. https://doi.org/10.1038/nature12957

Giglio, L., Boschetti, L., Roy, D., Hoffmann, A. A., Humber, M., & Hall, J. V. (2018). *Collection 6 MODIS Burned Area Product User's Guide Version 1.2*. Retrieved from http://modis-fire.umd.edu/files/MODIS_C6_BA_User_Guide_1.2.pdf

Giglio, L., Randerson, J. T., & van der Werf, G. R. (2013). Analysis of daily, monthly, and annual burned area using the fourth-generation global fire emissions database (GFED4). *Journal of Geophysical Research: Biogeosciences*, *118*(1), 317–328. https://doi.org/10.1002/jgrg.20042

Guyon, P., Frank, G. P., Welling, M., Chand, D., Artaxo, P., Rizzo, L., et al. (2005). Airborne measurements of trace gas and aerosol particle emissions from biomass burning in Amazonia. *Atmospheric Chemistry and Physics*, *5*(11), 2989–3002. https://doi.org/10.5194/acp-5-2989-2005

Heymann, J., Reuter, M., Buchwitz, M., Schneising, O., Bovensmann, H., Burrows, J. P., et al. (2017). $CO_2$ emission of Indonesian fires in 2015 estimated from satellite-derived atmospheric $CO_2$ concentrations. *Geophysical Research Letters*, *44*(3), 1537–1544. https://doi.org/10.1002/2016GL072042

Hubau, W., Lewis, S. L., Phillips, O. L., Affum-Baffoe, K., Beeckman, H., Cuní-Sanchez, A., et al. (2020). Asynchronous carbon sink saturation in African and Amazonian tropical forests. *Nature*, *579*(7797), 80–87. https://doi.org/10.1038/s41586-020-2035-0

Jiang, X., Camp, C. D., Shia, R., Noone, D., Walker, C., & Yung, Y. L. (2004). Quasi-biennial oscillation and quasi-biennial oscillation–annual beat in the tropical total column ozone: A two-dimensional model simulation. *Journal of Geophysical Research*, *109*(D16), D16305. https://doi.org/10.1029/2003JD004377

Jiang, X., Chahine, M. T., Olsen, E. T., Chen, L. L., & Yung, Y. L. (2010). Interannual variability of mid-tropospheric $CO_2$ from Atmospheric Infrared Sounder. *Geophysical Research Letters*, *37*(13), L13801. https://doi.org/10.1029/2010GL042823

Jiang, X., Wang, J. Q., Olsen, E. T., Pagano, T., Chen, L. L., & Yung, Y. L. (2013). Influence of stratospheric sudden warming on AIRS mid-tropospheric $CO_2$. *Journal of the Atmospheric Sciences*, *70*(8), 2566–2573. https://doi.org/10.1175/JAS-D-13-064.1

Kanamitsu, M., Ebisuzaki, W., Woollen, J., Yang, S.-K., Hnilo, J. J., Fiorino, M., & Potter, G. L. (2002). NCEP-DOE AMIP-II Reanalysis (R-2). *Bulletin of the American Meteorological Society*, *83*(11), 1631–1643. https://doi.org/10.1175/BAMS-83-11-1631(2002)083<1631:NAR>2.3.CO;2

Khanna, J., Medvigy, D., Fueglistaler, S., & Walko, R. (2017). Regional dry-season climate changes due to three decades of Amazonian deforestation. *Nature Climate Change*, *7*(3), 200–204. https://doi.org/10.1038/nclimate3226

Kulawik, S. S., Jones, D. B. A., Nassar, R., Irion, F. W., Worden, J. R., Bowman, K. W., et al. (2010). Characterization of Tropospheric Emission Spectrometer (TES) $CO_2$ for carbon cycle science. *Atmospheric Chemistry and Physics*, *10*(12), 5601–5623. https://doi.org/10.5194/acp-10-5601-2010

Levine, P. A., Randerson, J. T., Chen, Y., Pritchard, M. S., Xu, M., Hoffman, F. M. (2019). Soil moisture variability intensifies and prolongs eastern Amazon temperature and carbon cycle response to El Nino-Southern Oscillation. *Journal of Climate*, *32*(4), 1273–1292. https://doi.org/10.1175/JCLI-D-18-0150.1

Li, A. X., Wang, Y., & Yung, Y. L. (2019). Inducing factors and impacts of the October 2017 California wildfires. *Earth and Space Science*, *6*(8), 1480–1488. https://doi.org/10.1029/2019EA000661

Li, K.-F. (2018). An Intraseasonal Variability in $CO_2$ Over the Arctic Induced by the Madden–Julian Oscillation. *Geophysical Research Letters*, *45*(3), 1630–1638. https://doi.org/10.1002/2017GL076544

Li, K.-F., Tian, B., Waliser, D. E., & Yung, Y. L. (2010). Tropical mid-tropospheric $CO_2$ variability driven by the Madden–Julian oscillation. *Proceedings of the National Academy of Sciences of the United States of America*, *107*(45), 19171–19175. https://doi.org/10.1073/pnas.1008222107

Liu, J., Bowman, K. W., Schimel, D. S., Parazoo, N. C., Jiang, Z., Lee, M. et al. (2017). Contrasting carbon cycle responses of the tropical continents to the 2015–2016 El Nino. *Science*, *358*(6360), eaam5690. https://doi.org/10.1126/science.aam5690.

Marengo, J. A., Tomasella, J., Alves, L. M., Soares, W. R., & Rodriguez, D. A. (2011). The drought of 2010 in the context of historical droughts in the Amazon region. *Geophysical Research Letters*, *38*(12), L12703. https://doi.org/10.1029/2011GL047436

Nepstad, D., McGrath, D., Stickler, C., Alencar, A., Azevedo, A., Swette, B., et al. (2014). Slowing Amazon deforestation through public policy and interventions in beef and soy supply chains. *Science*, *344*(6188), 1118–1123. https://doi.org/10.1126/science.1248525

Pan, Y., Birdsey, R. A., Fang, J., Houghton, R., Kauppi, P. E., Kurz, W. A., et al. (2011). A large and persistent carbon sink in the world's forests. *Science*, *333*(6045), 988–993. https://doi.org/10.1126/science.1201609

Pastorello, G., Trotta, C., Canfora, E., Chu, H., Christianson, D., Cheah, Y.-W., et al. (2020). The FLUXNET2015 dataset and the ONEFlux processing pipeline for eddy covariance data. *Scientific data*, *7*(1), 225. https://doi.org/10.1038/S41597-020-0534-3

Randerson, J. T., Thompson, M. V., Malmstrom, C. M., Field, C. B., & Fung, I. Y. (1996). Substrate limitations for heterotrophs: Implications for models that estimate the seasonal cycle of atmospheric $CO_2$. *Global Biogeochemical Cycles*, *10*(4), 585–602. https://doi.org/10.1029/96GB01981

Randerson, J. T., van der Werf, G. R., Giglio, L., Collatz, G. J., & Kasibhatla, P. S. (2018). *Global Fire Emissions Database, Version 4.1 (GFEDv4)*. Oak Ridge, Tennessee, USA: ORNL DAAC. Retrieved from https://doi.org/10.3334/ORNLDAAC/1293

Rinsland, C. P., Chiou, L. S., Boone, C., & Bernath, P. (2010). Carbon dioxide retrievals from Atmospheric Chemistry Experiment solar occultation measurements. *Journal of Geophysical Research*, *115*(D3), D03105. https://doi.org/10.1029/2009JD012081

Schwandner, F. M., Gunson, M. R., Miller, C. E., Carn, S. A., Eldering, A., Krings, T., et al. (2017). Spaceborne detection of localized carbon dioxide sources. *Science*, *358*(6360), eaam5782. https://doi.org/10.1126/science.aam5782

Shiomi, K., Kawakami, S., Kina, T., Mitomi, Y., Yoshida, M., Sekio, N., et al. (2008). GOSAT level 1 processing and in-orbit calibration plan. Proceedings of SPIE 7106, Sensors, Systems, and Next-Generation Satellites XII (Vol. 7106, p. 71060O). International Society for Optics and Photonics. Retrieved from https://doi.org/10.1117/12.800278

Simonet, G., Subervie, J., Ezzine-de-Blas, D., Cromberg, M., & Duchelle, A. E. (2019). Effectiveness of a REDD+ Project in reducing deforestation in the Brazilian Amazon. *American Journal of Agricultural Economics*, *101*(1), 211–229. https://doi.org/10.1093/ajae/aay028

Soares-Filho, B., Rajão, R., Macedo, M., Carneiro, A., Costa, W., Coe, M., et al. (2014). Cracking Brazil's Forest Code. *Science*, *344*(6182), 363–364. https://doi.org/10.1126/science.1246663

Trenberth, K. E., Dai, A., van der Schrier, G., Jones, P. D., Barichivich, J., Briffa, K. R., & Sheffield, J. (2014). Global warming and changes in drought. *Nature Climate Change*, *4*(1), 17–22. https://doi.org/10.1038/nclimate2067

Walker, W. S., Gorelik, S. R., Baccini, A., Aragon-Osejo, J. L., Josse, C., Meyer, C., et al. (2020). The role of forest conversion, degradation, and disturbance in the carbon dynamics of Amazon indigenous territories and protected areas. *Proceedings of the National Academy of Sciences of the United States of America*, *117*(6), 3015–3025. https://doi.org/10.1073/pnas.1913321117

Wang, J., Jiang, X., Chahine, M. T., Liang, M.-C., Olsen, E. T., Chen, L. L., et al. (2011). The influence of tropospheric biennial oscillation on mid-tropospheric $CO_2$. *Geophysical Research Letters*, *38*(20), L20805. https://doi.org/10.1029/2011GL049288

Warner, J., Carminati, F., Wei, Z., Lahoz, W., & Attié, J. L. (2013). Tropospheric carbon monoxide variability from AIRS under clear and cloudy conditions. *Atmospheric Chemistry and Physics*, *13*(24), 12469–12479. https://doi.org/10.5194/acp-13-12469-2013

Wunch, D., Wennberg, P. O., Osterman, G., Fisher, B., Naylor, B., Roehl, C. M., et al. (2017). Comparisons of the Orbiting Carbon Observatory-2 (OCO-2) $X_{CO2}$ measurements with TCCON. *Atmospheric Measurement Techniques*, *10*(6), 2209–2238. https://doi.org/10.5194/amt-10-2209-2017

Yurganov, L. N., McMillan, W. W., Dzhola, A. V., Grechko, E. I., Jones, N. B., & van der Werf, G. R. (2008). Global AIRS and MOPITT CO measurements: Validation, comparison, and links to biomass burning variations and carbon cycle. *Journal of Geophysical Research: Atmospheres*, *113*(D9), D09301. https://doi.org/10.1029/2007JD009229